CYCLIC OUT-OF-PLANE BEHAVIOUR OF POST-TENSIONED CLAY BRICK MASONRY

Najif Ismail[1], Peter T. Laursen[2], Arturo E. Schultz[3] and Jason M. Ingham[4]

Abstract

Out-of-plane flexural testing of three (03) full scale unreinforced masonry (URM) walls seismically retrofitted using post-tensioning is reported. The selected wall configurations were representative of common URM walls that were vulnerable to out-of-plane failure, and imitated heritage URM construction by using salvaged clay brick masonry and ASTM type O mortar. Varying levels of pre-compression were applied to the test walls using a single mechanically restrained tendon inserted into a cavity at the centre of each test wall. Behaviour of the post-tensioned URM walls was compared to the response of a non-retrofitted URM wall, with the out-of-plane flexural strength of the post-tensioned masonry walls observed to range from 2.9 to 10.3 times the strength of the non-retrofitted URM wall. Several aspects pertaining to the seismic behaviour of post-tensioned masonry walls were investigated, including tendon stress variation, damage patterns, force-displacement behaviour, initial stiffness, and displacement capacity. Test results were compared with equations developed in previous studies, and it was established that the walls that were post-tensioned using seven-wire strands had measured strengths that compared favourably with predicted values, whereas the wall that was post-tensioned using mild steel bar had failed at a lower measured strength than the predicted value.

Keywords: post-tensioning, seismic retrofit, out-of-plane, structural masonry, clay brick

[1] Postgraduate Research Student, University of Auckland, Dept. of Civil and Env. Eng., Private Bag 92019, Auckland, 1142, New Zealand, nism009@aucklanduni.ac.nz
[2] Assistant Prof., California Polytechnic State University, Dept. of Arch. Eng., San Luis Obispo, California, 93407, USA, plaursen@calpoly.edu
[3] Prof., University of Minnesota, Dept. of Civil Eng., 500 Pillsbury Dr. SE, Minneapolis, MN, 55455, USA, schul088@umn.edu
[4] Associate Prof., University of Auckland, Dept. of Civil and Env. Eng., Private Bag 92019, Auckland, 1142, New Zealand, j.ingham@auckland.ac.nz

Introduction

The majority of fatalities caused by earthquakes in the last one hundred years have resulted from the collapse of unreinforced masonry (URM) buildings [Coburn and Spence 1992]. Poor seismic performance of URM buildings was also observed in recent earthquakes such as the 2005 M7.6 Pakistan earthquake [Ismail 2008; Bothara and Hicisyilmaz 2008], the 2008 M7.9 Sichuan earthquake [Zhao et al. 2009], the 2009 M5.8 L'Aquila earthquake [Kaplan et al. 2010] and the 2010 M7.1 Darfield earthquake [Ismail et al. 2011]. These experiences have highlighted the vulnerability of URM buildings to damage in the event of a large earthquake and the seismic hazard posed to their occupants. The two options available to alleviate these risks posed are either demolition, or the implementation of seismic retrofit to improve earthquake response. But important concerns associated with heritage preservation make demolition of these historic URM buildings undesirable, resulting in their seismic retrofit being preferred.

During large earthquakes URM walls are subjected to out-of-plane and/or in-plane lateral loading as well as vertical compression due to self weight and overburden loads. The self weight creates out-of-plane bending and due to their low tensile strength, URM walls having a height to thickness ‘h/t’ ratio greater than 14 are prone to out-of-plane flexural failure [Ewing and Kariotis 1981; Green 1993; Rutherford and Chekene 1990]. One method to improve the seismic performance of these out-of-plane loaded unstable URM walls is to apply vertical post-tensioning [Al-Manaseer and Neis 1987; Ganz and Shaw 1997; Laursen and Ingham 2004; Laursen et al. 2006; Rosenboom and Kowalsky 2004; Wight and Ingham 2008; Wight et al. 2006; Wight et al. 2007]. Research and codification of post-tensioned masonry originated from Switzerland and the United Kingdom, and over the last two decades significant research and development was led to multiple design code drafts [such as MSJC 2005; NZS 2004], but current design procedures for the seismic retrofit of URM walls using post-tensioning merit further research attention [Bean Popehn et al. 2008]. The performance of post-tensioned URM walls depends upon the initial post-tensioning force, tendon type and spacing, restraint conditions, and confinement. Post-tensioning can either be bonded when tendons are fully restrained, by grouting the cavity, or left unbonded by leaving cavities unfilled. Lateral restraint of post-tensioning tendons is important when considering second-order effects. Typically, additional axial load exacerbates bending stresses in URM walls as they displace due to P-Δ effects, whereas ensuring that tendons are laterally restrained eliminates additional P-Δ effects because the line of action of the post-tensioning load does not change with respect to the neutral axis of the wall [Ganz and Shaw 1997]. Because unbonded post-tensioning is reversible to some extent and has minimal impact on the architectural fabric of a building, the technique is deemed to be a desirable retrofit solution for URM buildings having important heritage value [Goodwin et al. 2009].

Experimental Program

Test wall details are specified in Table 1, with two post-tensioned walls (PTB-01 and PTS-02) having the same geometric configuration as that of a non-retrofitted wall C-01, and the third post-tensioned wall PTS-03 (series 2) having a configuration that matched the typical wall height found in commercial URM buildings. The selected wall configurations were representative of common out-of-plane loaded URM walls, achieving a low percentage of

new building strength when evaluated using the New Zealand Society for Earthquake Engineering guidelines [NZSEE 2006]. Recycled solid clay bricks, salvaged from an old URM building, and ASTM type O hydraulic cement mortar were used to imitate existing New Zealand and west coast USA URM construction. For post-tensioning of these three URM walls, a threaded mild steel bar and two different types of seven wire strand were tensioned with an initial applied force of 50 kN, 100 kN and 91 kN, corresponding to masonry axial stresses of 0.19 MPa, 0.39 MPa and 0.40 MPa. As maximum stresses develop at mid-height (hinge zone) when slender vertically spanning URM walls are subjected to out-of-plane seismic excitations, a single prestress tendon with bearing plates is adequate to produce the required stresses in the hinge zone by distributing axial compression stress at an angle of 45^o from the anchorage and into the wall. Therefore, all test walls were prestressed using one post-tensioned tendon (threaded bar or strand) inserted at the centre of the wall, and steel bearing plates were used to avoid localized masonry crushing.

Table 1. Wall Dimensions and Properties

Series	Wall	Effective height h_e (mm)	Length b (mm)	Thickness t (mm)	Tendon type	Initial prestress P_e (kN)	Initial prestress f_{se} (MPa)	Wall self-weight P_{sw} (kN)	Pre-compression (MPa)	Masonry strength f'_m (MPa)	Bearing stress f_m^a/f'_m (ratio)
1	C-01	3900	1170	220	-	-	-	19.0	0.00	10.7	-
1	PTB-01	3900	1170	220	B[b]	50	442	19.0	0.19	10.7[e]	0.32
1	PTS-02	3900	1170	220	S[c]	78.5	789	19.0	0.39	10.7[e]	0.56
2	PTS-03	3366	1090	210	S[d]	90.5	917	15.6	0.40	8.7	0.54

[a]$f_m=(P_e)/(A_n)$ where A_n is the area of bearing plate; [b]threaded mild steel bar (500 MPa); [c]sheathed, greased high strength seven-wire strand (1300 MPa); [d]sheathed, greased high strength seven-wire strand (1675 MPa); [e]constructed using masonry materials similar to C-01 and built at the same time

Test walls were constructed using a common bond pattern, with one header course after every three stretcher courses for wall series 1 and after every 5 stretcher courses for wall series 2, by an experienced brick layer under supervision. Salvaged solid clay bricks (230 mm × 110 mm × 90 mm for wall series 1 and 220 mm × 110 mm × 90 mm for wall series 2), were laid with roughly 15 mm thick mortar courses. A flexible 50 mm conduit was used to provide a cavity in the walls during construction and bricks were accordingly chiselled to accommodate the conduit. As there was no bond between masonry and tendon, the conduit encased tendon behaved as if it was placed in a cored cavity. From discussions with specialised local construction contractors it was established that for the seismic retrofit of URM buildings, current techniques are capable of drilling a core cavity up to 12 m with a precision of ±10 mm. Figure 1 shows a photograph of a coring operation being performed in Auckland on a heritage URM building.

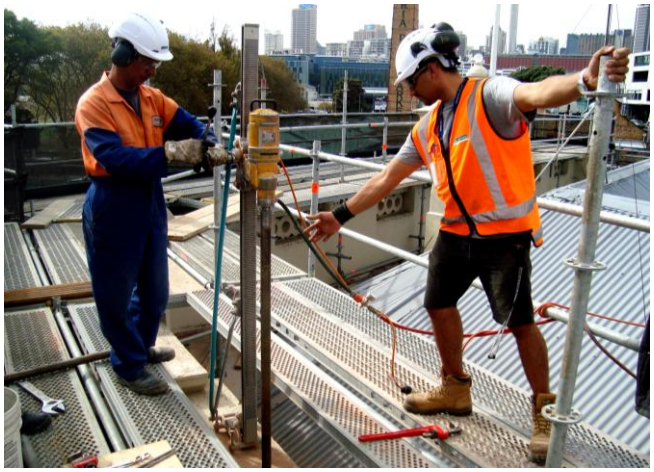

Figure 1. Coring Operation

Test wall PTB-01 was post-tensioned using a 100 kN hydraulic jack which was removed after tightening of the nut that clasped the post-tensioning bar. For test walls PTS-02 and PTS-03 a hydaulic jack was used to apply the initial post-tensioning force and the taut strand was clapsed by wedge interlocking. Post-tensioning losses and masonry creep are important factors that will inherently influence the design and longevity of an adequate retrofit. Testing by [Krause et al. 1996] briefly investigated prestress losses occurring in post-tensioned clay brick masonry walls over a span of 180 days, and found that losses were mainly attributable to the use of low-strength post-tensioning threaded steel bars, whereas modern anchorages and low-relaxation strands like those used for PTS-02 and PTS-03 have been proven to result in much smaller losses [Ganz and Shaw 1997]. The prestress levels detailed previously were ensured by applying the required stress immediately before testing.

Material Properties

Average URM material properties were determined by material testing consistent with standardised procedures [AS/NZS 2003; ASTM 2002; ASTM 2003; ASTM 2004], typically in samples of three. Masonry compressive strength f'_m and masonry elastic modulus E_m were determined by testing three brick high prisms, and mortar compressive strength f'_j was determined by testing three 50 mm × 50 mm cubes subjected to compression loading. Brick compressive strength f'_b was established using half brick specimens. Masonry cohesion C and coefficient of friction μ were investigated by bed joint shear testing of 6 three bricks high prisms that were subjected to varying magnitudes of axial compression applied using external post-tensioned high strength bars. To transfer prestress to the URM wall, end anchors (flat base hexagonal nuts for threaded bar and standard steel barrel anchors with wedges for the strand) were locked off onto steel plates (each being 220 mm × 220 mm × 50 mm) at the top and bottom of the wall. In order to make post-tensioning reverisble i.e., to remove the strand, a 40 mm thick mild steel plate split in two halves was used, which was removeable to destress the tendon once testing was concluded. Proof testing of each batch of tendons was perfomed by the supplier and the specified properties are reported in Table 2. Table 2 reports the material properties.

Table 2. Material Properties

Masonry Materials

Series		f'_b MPa	f'_j MPa	f'_m MPa	f_r MPa	C MPa	μ
1	Value	39.4	1.4	10.7	0.09	0.1	0.47
	COV	28%	8%	33%	29%	-	-
2	Value	-	-	8.7	0.28	-	-
	COV	-	-	9%	5%	-	-

where f'_b = brick compressive strength; f'_j = mortar compressive strength; f'_m = masonry compressive strength; f_r = tensile strength of masonry; C = mortar cohesion; and μ = coefficient of internal friction

Specified Tendon Properties

Series	Wall	D mm	A_{ps} mm^2	f_y MPa	f_u MPa	E_s GPa	Tendon Type
1	PTB-01	12.0	113.1	500	680	186	B
1	PTS-02	12.7	98.7	1680	1860	190	S
2	PTS-03	12.7	98.7	1680	1860	197	S

where D = diameter of the tendon; f_y = 2% nominal specified tensile yield strength; f_u = ultimate tensile strength; E_s = modulus of elasticity for steel; B = mild steel threaded bar; and S = sheathed seven wire strand

Wall Boundary Conditions

The selected configurations were representative of the most prevalent storey heights found in historic URM buildings. Vertically spanning face-loaded URM walls are known to remain linearly elastic until cracking initiates, after which upper and lower segments rotate about the

hinge that forms at wall mid-height [Bean Popehn et al. 2008; Doherty et al. 2002]. Therefore, simply supported boundary conditions were used in the test setup and the level of pre-compression applied to the wall (see Table 1) was representative of a typical scenario where stresses would be attributed to both overburden compression due to upper storeys and compression due to prestress. The boundary conditions and the rotational restraints applied to the test wall were similar to those used in previous studies on out-of-plane loaded walls [Bean Popehn et al. 2008; Doherty et al. 2002].

Testing Details

Testing of the post-tensioned walls PTB-01 and PTS-02 was conducted using the air bag rig shown in Figure 2a, consisting of steel sections supporting a plywood backing frame, a rigid steel reaction frame anchored to the concrete floor, air bags capable of withstanding 15 kPa air pressure, air compressor, four S shape two volt load cells, frictionless plates, six steel clamps, steel connecting rods to connect load cells to the reaction frame, and a linear variable differential transducer with stand. Air bags were used to apply a uniformly distributed pseudo-static load, emulating a lateral seismic load generated in the out-of-plane direction. The backing frame was placed over two greased steel plates having negligible friction, such that the backing frame self weight did not impair the test results. When air bags were inflated using the air compressor, the backing frame exerted force to load cells measuring the applied load on the test wall. The rigid reaction frame acted as a backing and also supported the top of the wall, creating boundary conditions comparable to those when a post-tensioned wall is connected to a floor or ceiling diaphragm.

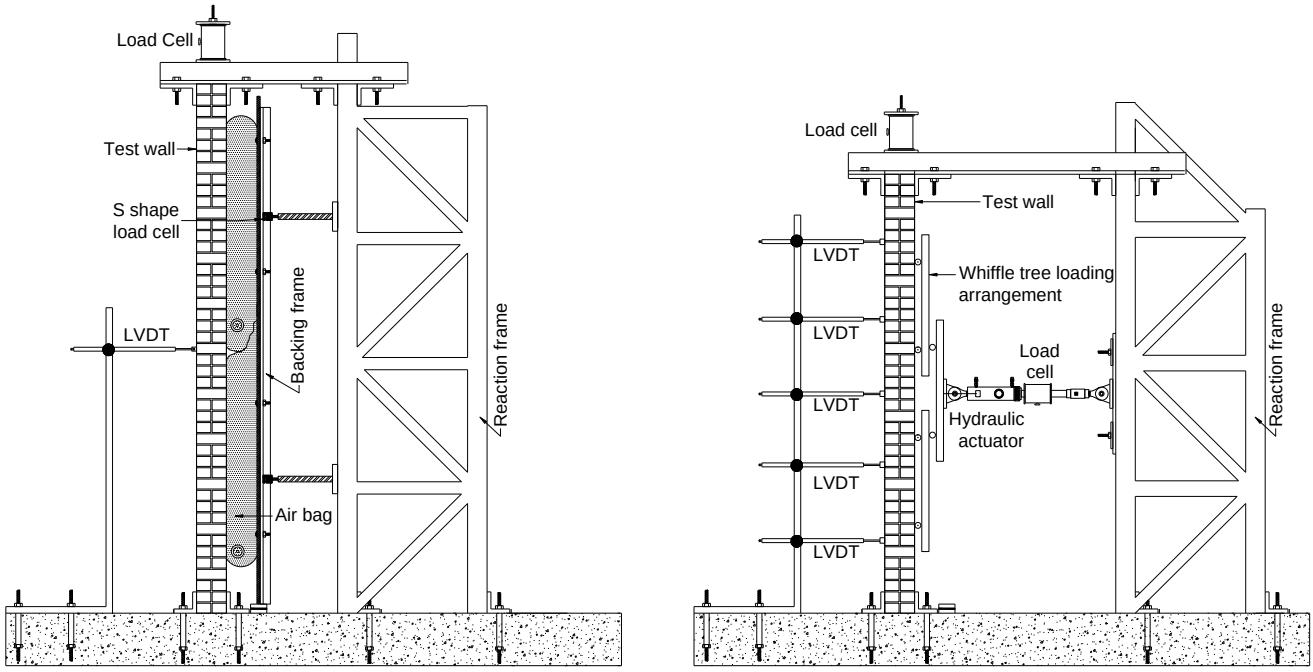

(a) Series 1 (b) Series 2

Figure 2. Test Setup

Displacement controlled loading cycles were applied by inflating and deflating the air bags. The third test wall PTS-03 was tested with the same setup, but used a whiffle tree loading system to simulate uniform lateral loading, along with a load cell to measure the force magnitude applied (see Figure 2b). This whiffle tree setup enabled the application of more frequent load cycles and deflection of the test wall to larger displacements than could be achieved using an air bag rig. For all post-tensioned walls a load cell was located between the tendon anchorage and the top of the wall, to record the force in the post-tensioning tendon. For series 1 testing, one linear variable differential transducer (LVDT) was located at wall mid-height to determine lateral displacement and four S shape 2 volt load cells were used to determine the force applied by air bags. For series 2 testing, the total lateral force applied to the wall was recorded between the hydraulic ram and the steel load spreader using a 220 kN load cell, and six LVDTs were located at five equally spaced points on the tension face of the wall, with two LVDTs at mid-height to determine whether any wall twisting occurred.

Test Results

In order to interpret the seismic behaviour of the tested post-tensioned masonry walls, five different damage levels, adapted from a previous study [Bean Popehn et al. 2008], were defined on the force-displacement envelope of each wall. The defined damage levels represent five base shear values numbered 1 to 5, where 1 = measured value when the first crack appeared in the test wall and corresponds to performance in the elastic range; 2 = measured value when upper and lower wall segments started to rotate; 3 = predicted nominal strength; 4 = measured ultimate strength; and 5 = measured value when post-peak strength degraded to $0.8V_u$. Quantification of initial stiffness is important when modelling the dynamic response of a post-tensioned URM wall. The wall secant stiffness at or near first cracking varied for the test walls. However, the initial average stiffness was quantified as the secant modulus between $0.05V_u$ and $0.75V_u$ (see K_i in Table 3). Flexural capacities at first cracking and nominal strength levels were predicted using Equations 1 and 2 [Bean Popehn et al. 2008], and the input parameters and performance of test walls are summarized in Table 3. The ultimate displacement capacity was defined as $\gamma_u = 2d_u/h_e$, where d_u = displacement corresponding to failure (corresponding to damage level 5).

$$M'_c = \frac{I_n}{c}\left[f_r + \left(\frac{P_v + P_{sw} + A_{ps}f_{se}}{A_n}\right)\right] \quad (1)$$

$$M_n = \left(P_v + P_{sw} + A_{ps}f_{se}\right)\left[d_{eff} - \frac{\left(P_v + P_{sw} + A_{ps}f_{se}\right)}{2\left(\lambda_n f'_m b\right)}\right] \quad (2)$$

Test wall PTB-01 was loaded until its post-peak strength degraded to nearly half of the measured flexural strength, but test walls PTS-02 and PTS-03 did not reach their predicted flexural capacity before the test was stopped due to safety concerns. In test wall PTB-01 the threaded mild steel bar reached its elastic limit and yielded, causing strength degradation, but no visible residual deflections were observed. A ductile and nonlinear elastic behaviour was observed in walls PTS-02 and PTS-03, with strand stress not exceeding the specified elastic

limit and the wall returning to its original position. This nonlinear elastic behaviour was attributed to the self centring behaviour of post-tensioned masonry.

Table 3. Test Results

Input parameters for predictive equations														
Series	Wall	P_v kN	P_{sw} kN	A_{ps} mm^2	f_{se} MPa	b mm	P_e kN	c mm	d_{eff} mm	A_n m^2	I_n m^4	f_r MPa	f'_m MPa	λ_n -
1	C-01	0	19.0	-	-	1170	-	110	110	0.26	0.001	0.09	10.7	0.85
1	PTB-01	0	19.0	113.1	442	1170	50	110	110	0.26	0.001	0.09	10.7	0.85
1	PTS-02	0	19.0	98.7	789	1170	78.5	110	110	0.26	0.001	0.09	10.7	0.85
2	PTS-03	0	15.6	98.7	717	1090	90.5	110	110	0.24	0.001	0.28	8.7	0.85

Test results and comparison with predicted values													
Series	Wall	Predicted values				Actual values				γ_u	V_c/V'_c	V_u/V_n	K_i
		V'_c (kN)	V_n (kN)	M'_c (kN.m)	M_n (kN.m)	V_c (kN)	V_u (kN)	M_c (kN.m)	M_u (kN.m)	(%)	(%)	(%)	
1	C-01	3.0	-	1.5	-	2.2	2.2	1.1	1.1	3	73%	-	1.3
1	PTB-01	6.6	12.8	3.3	7.4	4.6	6.3	2.3	3.2	1.6	70%	43%	3.0
1	PTS-02	8.8	20.6	4.4	10.3	10.8	>12.3	5.4	>6.2	>4.4	123%	-	3.1
2	PTS-03	12.8	22.0	6.4	11.0	14.5	26.4	7.2	13.2	7.9	113%	120%	5.0

where I_n = net moment of inertia of the wall; c = distance from extreme compression fibre to neutral axis; f_r= modulus of rupture; P_v= overburden axial load due to upper storeys; P_{sw} = axial load due to self weight; A_{ps} = area of post-tensioning steel; f_{se} = effective stress in tendon (calculated after deducting the prestress losses); P_e = effective post-tensioning force (and $P_e = A_{ps}f_{ps}$); A_n = net cross sectional area of the masonry; d_{eff} = distance from extreme compression fibre to centroid of tendon; f'_m = compressive strength of masonry; b = width of the wall tributary to one tendon; λ_n = parameter representing the fraction of maximum compressive stress at nominal strength; M'_c = predicted flexural strength at first cracking; V_c = predicted lateral force at first cracking; M_n = predicted nominal flexural strength; V_n = predicted ultimate lateral force; M_c = measured flexural strength when first crack appeared; V_c = measured lateral force at first cracking; M_u = measured ultimate flexural strength; V_u = measured maximum lateral force; γ_u= ultimate displacement capacity, and K_i = initial stiffness of the wall

A single large crack at or near mid-height was observed in all tests, with no distributed flexural cracking, and upon increasing the applied lateral load this horizontal crack started to widen. The maximum opening of the crack noted was 18 mm in PTS-03 at the maximum mid-height displacement of 201 mm, and similar behaviour was observed in the other tests. All force-displacement histories (see Figure 4) were plotted with analogous moment and drift values on a secondary axis to allow comparison between the results of test walls having different heights. Figure 3(a) shows a photograph of a deflected test wall and Figure 3(b) shows the corresponding deformed wall geometry.

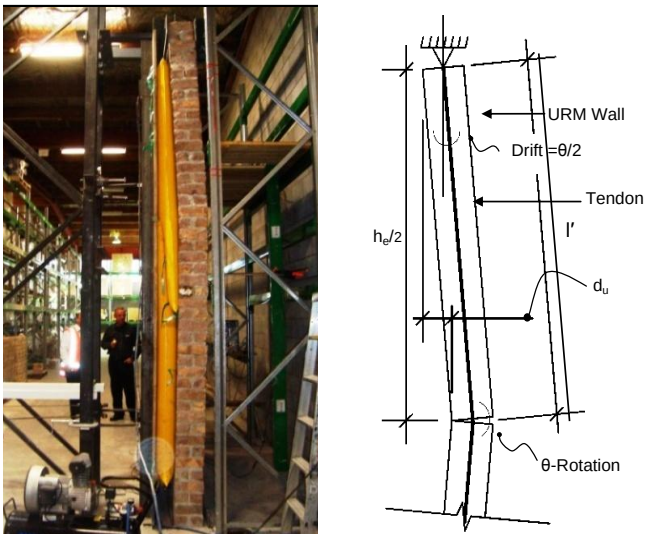

(a) Photograph of wall test (b) Deformed wall geometry

Figure 3. Deflected Test Wall

Force-Displacement Response

Figures 4(a), 4(b), 4(d) and 4(f) show the measured force-displacement response for walls CO-01, PTB-01, PTS-02 and PTS-03 respectively. The negatively sloped post peak force-displacement behaviour of PTB-01 is due to yielding of the mild steel post-tensioning bar, with similar behaviour previously reported in [Bean Popehn et al. 2008] and [Lacika and

Drysdale 1995]. In order for retrofitted walls to exhibit ductile behaviour, the restoring force provided by the tendon must be maintained after excursions to large lateral displacements of the wall and design must ensure that the increased tendon stress during these excursions does not exceed the tendon yield strength. An initial tendon stress of $0.55f_{pu}$ is recommended in [NZS 2004], where f_{pu} is the rupture stress of the tendon. Positively sloped post cracking behaviour was observed for walls PTS-02 and PTS-03, attributed to the prestressing strand not exceeding its elastic limit even at large displacement values. A comparison of the force-displacement histories for the series 1 test walls indicated that the nominal out-of-plane flexural strength of test walls PTB-01 and PTS-02 was respectively 2.9 times and 10.3 times the strength of the non-retrofitted URM wall. Test walls PTS-02 and PTS-03 exhibited larger flexural capacity, larger pseudo-ductility values and showed minimal contribution from masonry towards the flexural strength than did wall PTB-01.

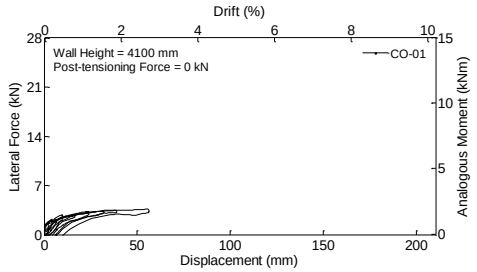

(a) Force-displacement response for CO-01

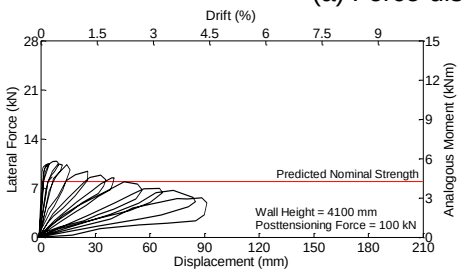

(b) Force-displacement response for PTB-01

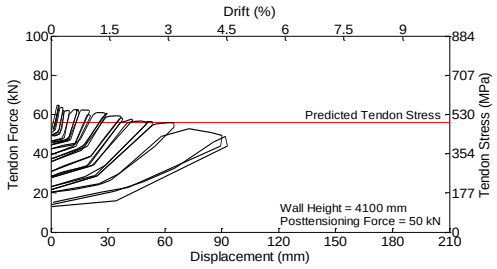

(c) Tendon stress plot for PTB-01

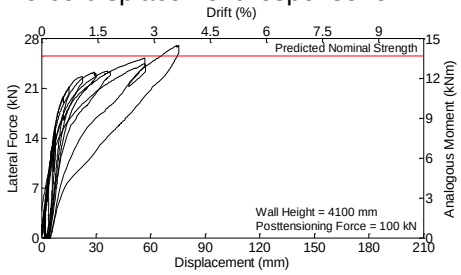

(d) Force-displacement response for PTS-02

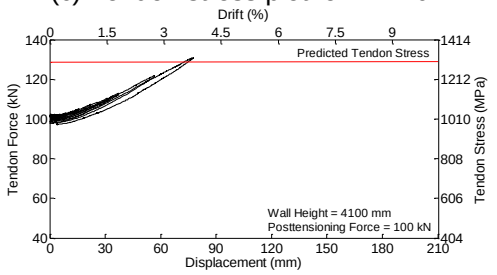

(e) Tendon stress plot for PTS-02

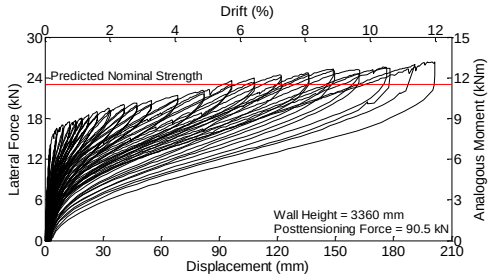

(f) Force-displacement response for PTS-03

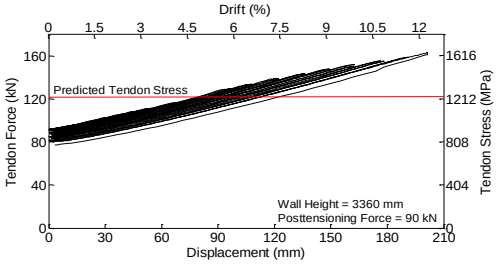

(g) Tendon stress plot for PTS-03

Figure 4. Test Results

Tendon Stress

Figures 4(c), 4(e) and 4(g) show the tendon stress histories plotted against the lateral displacement at hinge location. For wall PTB-01 the tendon stress reached its yield strength at 14 mm lateral displacement, and once the bar had yielded the maximum tendon force was reduced during subsequent loading cycles. For wall PTS-02 the strand stress increased linearly and remained well within its elastic limit, with no observed signs of strength degradation in the wall. For wall PTS-03 the strand remained elastic with a maximum stress increase of nearly 40% of its initial stress, and with minor stress loss observed following the conclusion of testing to large displacement excursions.

Conclusions

Three post-tensioned URM walls, having different types of tendons, were structurally tested to evaluate a number of characteristics related to their out-of-plane seismic behaviour. Masonry materials used were salvaged clay bricks and a hydraulic cement mortar, having strength characteristics similar to those found in typical URM buildings, and were determined using standardised test procedures. Test walls having two typical geometric characteristics were subjected to one directional out-of-plane simulated seismic cyclic loading. A single crack at hinge location was observed in all tests. Self centring response of post-tensioned URM walls was observed, which is advantageous for enabling immediate occupancy after an earthquake. Nonlinear elastic behaviour was observed for test walls post-tensioned using strands (where strand stress did not exceed its tensile yield strength), whereas strength degradation attributed to tensile yielding of the bar was observed in the wall that was post-tensioned using a threaded mild steel bar. Total lateral force corresponding to first cracking and ultimate strength levels were determined and were compared to the predicted values. It was inferred that existing equations previously establishing flexural capacity provided good predictions for walls PTS-02 and PTS-03, but that the flexural strength of wall PTB-01was lower than predicted.

Acknowledgement

This research was conducted with financial support from the New Zealand Foundation for Research, Science and Technology and from Reid Construction Systems. The Higher Education Commission of Pakistan provided funding for the doctoral studies of the first author. The authors thank Derek Lawley, Terry Seagrave, Daniel Lazzarini and Tek Goon Ang for assisting with the experimental program.

References

Al-Manaseer and Neis 1987: Al-Manaseer A. A, and V. V. Neis, “Load Tests on Post-tensioned Masonry Wall Panels”, ACI Structural Journal, 84(3), 1987, pp.467-472.

AS /NZS 2003: AS/NZS. "AS/NZS 4456.15: Masonry Units and Segmental Pavers and Flags, Methods of Test, Determining Lateral Modulus of Rupture", Standards Australia, Sydney NSW 2001, Australia, 2003.

ASTM 2002: ASTM. "ASTM C109/C109M-02: Standard Test Method for Compressive Strength of Hydraulic Cement Mortars", American Society for Testing and Materials International, West Conshohoken, Pa, USA, 2002.

ASTM 2003: ASTM. "ASTM C270-03: Standard Test Method for Compressive Strength of Masonry Prisms", American Society for Testing and Materials International, West Conshohoken, Pa, USA, 2003.

ASTM 2004: ASTM. "ASTM C62-04: Standard Specification for Building Brick- Solid Masonry Units Made from Clay or Shale", American Society for Testing and Materials International, West Conshohoken, Pa, USA, 2004.

Bean Popehn et al. 2008: Bean Popehn J. R, A. E. Schultz, M. Lu, H. K. Stolarski and N. J. Ojard. "Influence of Transverse Loading on the Stability of Slender Unreinforced Masonry Walls", Engineering Structures, 30(10), 2008, pp. 2830-2839.

Bothara and Hicisyilmaz 2008: Bothara J. K and K. M. O. Hicisyilmaz, "General Observations of Building Behaviour during the 8th October 2005 Pakistan Earthquake", Bulletin of the New Zealand Society for Earthquake Engineering, 41(4), 2008, pp. 209-233.

Coburn and Spence 1992: Coburn A and R. Spence, Earthquake Protection. Willey, New York, USA, 1992.

Doherty et al. 2002: Doherty K, M. C. Griffith, N. Lam, and J. Wilson (2002). "Displacement-Based Seismic Analysis for the Out-Of-Plane Bending of Unreinforced Masonry Walls", Earthquake Engineering and Structural Dynamics, 31(4), 2002, pp. 833-850.

Ewing and Kariotis 1981: Ewing R. D, and J. C. Kariotis. "Methodology for Mitigation of Seismic Hazards in Existing Unreinforced Masonry Buildings: Wall Testing, Out-of-Plane", Topical report number 04, A Joint Venture of Agbabian Associates, S.B. Barnes and Associates and Kariotis and Associates (ABK), El Segundo, CA, 1981.

Ganz and Shaw 1997: Ganz H. R and G. Shaw. "Stressing Masonry's Future". Civil Engineering (New York), 67(1), 1997, pp. 42-45.

Goodwin et al. 2009: Goodwin C, G. Tonks and J. M. Ingham. "Identifying heritage value in URM buildings", Journal of the Structural Engineering Society of New Zealand, 22(2), 2009, pp. 16-28.

Green 1993: Green, M. "Code Provisions for Unreinforced Masonry Bearing Wall Buildings in California". Proceedings of the Symposium on Structural Engineering in Hazard Mitigation, American Society of Civil Engineers, Irvine CA, United States, 19-21 April 1993.

Ismail 2008: Ismail N. "Comparative Studies of IMRF and SMRF in Moderate Seismic Zones", Master's Thesis, University of Engineering and Technology, Taxila, Pakistan, 2008.

Ismail et al. 2011: Ismail N, M. Griffith, and J. M. Ingham, "Performance of Masonry Buildings during the 2010 Darfield (New Zealand) Earthquake", Proceedings of the 11th North American Conference, Minneapolis, USA, 5-8 June 2011.

Kaplan et al. 2010: Kaplan H, H. Bilgin, S. Yilmaz, H. Binici, and A. Aztas, "Structural Damages of L'Aquila (Italy) Earthquake", Natural Hazards and Earth System Science, 10(3), 2010, pp. 499-507.

Krause et al. 1996: Krause G. L, R. Devalapura and M. K. Tadros. "Testing of Prestressed Clay-Brick Walls", Proceedings of the ASCE Symposium in Conjunction with Structures Congress XIV, Chicago IL, USA, 15-18 April 1996.

Lacika and Drysdale1995 : Lacika E. M, and R. G. Drysdale. "Experimental Investigation of Slender Prestressed Brick Walls". Proceedings of the 7th Canadian Masonry Symposium, Hamilton Ontario, Canada, 4-7 June 1995.

Laursen and Ingham 2004: Laursen P. T, and J. M. Ingham. "Structural Testing of Large-Scale Post-tensioned Concrete Masonry Walls", Journal of Structural Engineering, 130(10), 2004, pp. 1497-1505.

Laurrsen et al. 2006: Laursen P. T, G. D. Wight and J. M. Ingham. "Assessing Creep and Shrinkage Losses in Post-tensioned Concrete Masonry", ACI Materials Journal, 103(6), 2006, pp. 427-435.

MSJC 2005: MSJC. "ACI 530-05/ASCE 5-05/TMS 402-05: Building Code Requirements for Masonry Structures and Specification for Masonry Structures", The Masonry Standards Joint Committee, USA, 2005.

NZS 2004: NZS. "NZS 4230-2004: Design of Reinforced Concrete Masonry Structures", Standards New Zealand, Wellington, New Zealand, 2004.

NZSEE 2006: NZSEE. "Assessment and Improvement of the Structural Performance of Buildings in Earthquakes: Prioritisation, Initial Evaluation, Detailed Assessment, Improvement Measures", New Zealand Society for Earthquake Engineering, Wellington, New Zealand, 2006.

Rosenboom and Kowalsky 2004: Rosenboom O. A and M. J. Kowalsky. "Reversed In-plane Cyclic Behavior of Post-tensioned Clay Brick Masonry Walls", Journal of Structural Engineering, 130(5), 2004, pp. 787-798.

Rutherford and Chekene 1990: Rutherford and Chekene. "Seismic Retrofitting Alternatives for San Francisco's Unreinforced Masonry Buildings: Estimates of Construction Cost and Seismic Damage for the San Francisco Department of City Planning", Rutherford and Chekene Consulting Engineer, San Francisco CA, USA, 1990.

Wight and Ingham 2008: Wight G. D and J. M. Ingham. "Tendon Stress in Unbonded Post-tensioned Masonry Walls at Nominal In-plane Strength". Journal of Structural Engineering, 134(6), 2008, pp. 938-946.

Wight et al. 2006: Wight G. D, J. M. Ingham and M. J. Kowalsky. "Shaketable Testing of Rectangular Post-tensioned Concrete Masonry Walls", ACI Structural Journal, 103(4), 2006, pp. 587-595.

Wight el at. 2007: Wight G. D, J. M. Ingham and A. R. Wilton. "Innovative Seismic Design of a Post-tensioned Concrete Masonry House", Canadian Journal of Civil Engineering, 34(11), 2007, pp. 1393-1402.

Zhao et al. 2009: Zhao T, X. Zhang, and Z. Tian, "Analysis of Earthquake Damage to Masonry School Buildings in Wenchuan Earthquake", World Information on Earthquake Engineering, 25(3), 2009, pp. 150-158.